ISSN 1001-0742
CN 11-2629/X

2012

Volume 24
Number 10

JOURNAL OF ENVIRONMENTAL SCIENCES

ELSEVIER
Science Press

Sponsored by
Research Center for Eco-Environmental Sciences
Chinese Academy of Sciences

JOURNAL OF ENVIRONMENTAL SCIENCES

(http://www.jesc.ac.cn)

Aims and scope

Journal of Environmental Sciences is an international academic journal supervised by Research Center for Eco-Environmental Sciences, Chinese Academy of Sciences. The journal publishes original, peer-reviewed innovative research and valuable findings in environmental sciences. The types of articles published are research article, critical review, rapid communications, and special issues.

The scope of the journal embraces the treatment processes for natural groundwater, municipal, agricultural and industrial water and wastewaters; physical and chemical methods for limitation of pollutants emission into the atmospheric environment; chemical and biological and phytoremediation of contaminated soil; fate and transport of pollutants in environments; toxicological effects of terrorist chemical release on the natural environment and human health; development of environmental catalysts and materials.

For subscription to electronic edition

Elsevier is responsible for subscription of the journal. Please subscribe to the journal via http://www.elsevier.com/locate/jes.

For subscription to print edition

China: Please contact the customer service, Science Press, 16 Donghuangchenggen North Street, Beijing 100717, China. Tel: +86-10-64017032; E-mail: journal@mail.sciencep.com, or the local post office throughout China (domestic postcode: 2-580).

Outside China: Please order the journal from the Elsevier Customer Service Department at the Regional Sales Office nearest you.

Submission declaration

Submission of an article implies that the work described has not been published previously (except in the form of an abstract or as part of a published lecture or academic thesis), that it is not under consideration for publication elsewhere. The submission should be approved by all authors and tacitly or explicitly by the responsible authorities where the work was carried out. If the manuscript accepted, it will not be published elsewhere in the same form, in English or in any other language, including electronically without the written consent of the copyright-holder.

Submission declaration

Submission of the work described has not been published previously (except in the form of an abstract or as part of a published lecture or academic thesis), that it is not under consideration for publication elsewhere. The publication should be approved by all authors and tacitly or explicitly by the responsible authorities where the work was carried out. If the manuscript accepted, it will not be published elsewhere in the same form, in English or in any other language, including electronically without the written consent of the copyright-holder.

Editorial

Authors should submit manuscript online at http://www.jesc.ac.cn. In case of queries, please contact editorial office, Tel: +86-10-62920553, E-mail: jesc@263.net, jesc@rcees.ac.cn. Instruction to authors is available at http://www.jesc.ac.cn.

Copyright

ISSN 1001–0742 **Journal of Environmental Sciences** Vol. 24 No. 10 2012

CONTENTS

Serial parameter: CN 11-2629/X*1989*m*162*en*P*20*2012-10

Available online at www.sciencedirect.com
ScienceDirect
Journal of Environmental Sciences 2012, 24(10) 1876–1884
JOURNAL OF ENVIRONMENTAL SCIENCES
ISSN 1001-0742
CN 11-2629/X
www.jesc.ac.cn

TiO_2/Ag modified penta-bismuth hepta-oxide nitrate and its adsorption performance for azo dye removal

Eshraq Ahmed Abdullah[2,*], Abdul Halim Abdullah[1,2], Zulkarnain Zainal[1,2], Mohd Zobir Hussein[1,2], Tan Kar Ban[2]

1. Advanced Material and Nanotechnology Laboratory, Institute of Advanced Technology, Universiti Putra Malaysia, 43400, UPM Serdang, Selangor, Malaysia
2. Department of Chemistry, Faculty of Science, Universiti Putra Malaysia, 43400, UPM Serdang, Selangor, Malaysia.
E-mail: yemenahmed2009@gmail.com

Received 08 November 2011; revised 29 April 2012; accepted 10 May 2012

Abstract

A modified hydrophilic penta-bismuth hepta-oxide nitrate ($Bi_5O_7NO_3$) surface was synthesized via a precipitation method using TiO_2 and Ag as modified agents. The synthesized product was characterized by different analytical techniques. The removal efficiency was evaluated using mono- and di-sulphonated azo dyes as model pollutants. Different kinetic, isotherm and diffusion models were chosen to describe the adsorption process. X-ray photoelectron spectroscopy (XPS) results revealed no noticeable differences in the chemical states of modified adsorbent when compared to pure $Bi_5O_7NO_3$; however, the presence of hydrophilic centres such as TiO_2 and Ag developed positively charged surface groups and improved its adsorption performance to a wide range of azo dyes. Dyes removal was found to be a function of adsorbent dosage, initial dye concentration, solution pH and temperature. The reduction of Langmuir 1,2-mixed order kinetics to the second or first-order kinetics could be successfully used to describe the adsorption of dyes onto the modified adsorbent. Mass transfer can be described by intra-particle diffusion at a certain stage, but it was not the rate limiting step that controlled the adsorption process. Homogenous behavior of adsorbent surface can be explored by applying Langmuir isotherm to fit the adsorption data.

Key words: $Bi_5O_7NO_3$; X-ray photoelectron spectroscopy; Langmuir 1,2-mixed order; azo dye; mass transfer

DOI: 10.1016/S1001-0742(11)60994-7

Introduction

Colour as an indicator of visual pollution in wastewater has drawn considerable attention among environmental scientists in the last few decades (Anjaneyulu et al., 2005). Paper, pharmaceutical, textile and food industries use large quantities of water which result in the production of considerable amounts of coloured compounds in wastewater (Patel and Vashi, 2010). Among various visual pollutants, dye wastes are the predominant colouring agents in the food and textile industries (Andleeb et al., 2010).

Methyl Orange (MO) is not a carcinogenic dye; however, the aromatic reduction products of this dye are highly carcinogenic (Zbaida et al., 1989). Synthetic azo dye, Sunset Yellow (SY), is a colouring agent that is widely used in the food and drug industries as additives (Poul et al., 2009). The genotoxic effect of the SY dye has not been reported (Combes and Haveland-Smith, 1982); even though the discharge of these coloured wastes disturbs ecological balance of the water and inhibits photosynthesis (Guendy, 2010).

The decolourization of dye wastes is attracting growing attention in the domain of adsorption science. Activated carbon a commonly used adsorbent; however, due to high cost, its application for coloured compound removal is restricted. In addition, the low efficiency of low-cost materials towards the organic pollutants has emphasised the need to synthesize and/or develop new suitable adsorbents for organic contaminant removal.

In academic and industrial research, the control of surface chemistry is a major technological driver in the development of adsorptive materials. Several techniques have been employed in an attempt to modify the surface chemistry of an adsorbent (Afkhami et al., 2010; El-Qada et al., 2008). The use of hydrophilic materials such as TiO_2 and Ag-TiO_2 to develop the surface chemistry and improve selective removal has been reported (Enomoto et al., 2002; Samokhvalov et al., 2010).

Penta-bismuth hepta-oxide nitrate, $Bi_5O_7NO_3$ as a layered structure of bismuth oxide is well known as an anion exchanger (Kodama, 1994a). The surface chemistry of $Bi_5O_7NO_3$ has been investigated in our previous research. However, attempts to control surface charged groups and clarify its relationship with the adsorption performance of

* Corresponding author. E-mail: yemenahmed2009@gmail.com

$Bi_5O_7NO_3$ have not been reported.

The present research attempts to modify $Bi_5O_7NO_3$ using different hydrophilic agents such as TiO_2 and/or Ag particles. The structure and surface chemistry of modified adsorbent were characterized. The potential use of the modified adsorbent was evaluated using a wide range of mono- and di-sulphonated azo dyes.

1 Materials and methods

1.1 Materials

The chemicals of different commercial brands were used without further purification. Bismuth nitrate penta-hydrate, $Bi(NO_3)_3{\cdot}5H_2O$ (98%) (Acros Organic, USA), nitric acid (65%) (Fisher Scientific, USA), and ammonium hydroxide, $NH_3{\cdot}H_2O$ (25%) (Merck, Germany) were used to synthesize $Bi_5O_7NO_3$ adsorbent. Titanium dioxide, TiO_2 (P25) (Evonik Degussa, Germany), and silver nitrate, $AgNO_3$ (Gerchem, Germany) were used to modify $Bi_5O_7NO_3$. Methyl Orange dye (MO, Sigma Aldrich, USA) and Sunset Yellow dye (SY, Aldrich, USA) were used as model pollutants. Nitric acid and sodium hydroxide were used to adjust the initial pH of the solution to predetermined levels. Deionised water was used in all experiments.

1.2 Synthesis of TiO_2, Ag and TiO_2-Ag modified $Bi_5O_7NO_3$ adsorbents

Modified $Bi_5O_7NO_3$ adsorbents with different modification systems including titanium dioxide and/or silver nitrate, were synthesized via a precipitation method by applying some modifications to the described method for pure $Bi_5O_7NO_3$ (Abdullah et al., 2012). Titanium dioxide, TiO_2 (0.125, 0.25 and 0.5 g), and/or silver nitrate, $AgNO_3$ (0.175 g), were added to a 20 mL concentrated nitric acid solution containing 10 g of $Bi(NO_3)_3{\cdot}5H_2O$. The suspension was aged with vigorous stirring for 30 min. Then, ammonium hydroxide (50%, V/V) was added to the suspension with continuous stirring until the pH of the solution reached 9. The mixture was aged again with vigorous stirring for 1 hr. The precipitate obtained was filtered, washed with distilled water and then dried overnight in an oven at 110°C. The precipitate was calcined at 450°C for 1 hr in an open horizontal tube furnace.

1.3 Characterization

The powder diffraction pattern was recorded in the 2θ range of 10°–70° with a scan speed of 0.05°/sec on a X'PERT-PRO diffractometer using Cu-K_α radiation. The thermal behavior and decomposition products were determined using thermogravimetric analysis (TGA). The TGA curve was recorded on a TGA/SDTA 851 Perkin Elmer thermal analyzer. The surface area and the pore size distribution were determined using Brunauer-Emmet-Teller (BET) and Barret-Joyer-Haenda (BJH) methods. The pH of the point of zero charge (pH_{pzc}) was determined by the batch equilibrium method described elsewhere (Fernandes et al., 2007). The XPS spectra were acquired at room temperature with an XPS AXIS ULTRA instrument using an Al-K_α (1486.6 eV) monochromatic radiation source. The TiO_2 loading on modified adsorbents was determined by an energy dispersive X-ray fluorescence spectrometer (XRF) (Shimadzu EDX-720). The concentration of Ag was determined by a Thermo Scientific S series atomic absorption spectrometer (AAS) using an air-acetylene flame at a wavelength of 328.1 nm.

1.4 Batch adsorption studies

Experiments were conducted in a 1000 mL beaker as the reaction vessel containing desired dye concentrations (10–40 mg/L) to which specific amounts of prepared adsorbents were added. The suspensions were mixed with a magnetic stirrer for 3 hr at 298 K. After a pre-determined time, the solution was separated by a 0.45 μm syringe filter, and the dye concentration was analyzed through a UV-1650 PC Shimadzu spectrophotometer at the maximum wavelength after appropriate dilution. The adsorption capacities of the adsorbent were reported as a function of the remaining dye concentration in the solution as follows:

$$q = (C_o - C_e)\frac{V}{m_s} \quad (1)$$

where, q (mg/g) is the amount of dye adsorbed onto a unit amount of the adsorbent, C_o (mg/L) and C_e (mg/L) are the initial and equilibrium total concentration of dye in the solution, respectively, V (L) is the volume of the solution, and m_s (g) is the dry weight of the adsorbent used. The effect of experimental parameters were studied at different adsorbent dosages (0.2–1.0 g), pH (3–10) and temperatures (298, 313 and 333 K). Each experiment was performed thrice for all parameters and average values were reported.

2 Results and discussion

2.1 Surface modification of $Bi_5O_7NO_3$

Surface modification of $Bi_5O_7NO_3$ adsorbent was performed using TiO_2 and/or $AgNO_3$ as modification agents. A comparison study between raw and modified $Bi_5O_7NO_3$ was made as presented in Fig. 1. The introduction of 0.125 g of TiO_2 particles (TB system) on the $Bi_5O_7NO_3$ surface increased the adsorption capacity of MO dye removal. However, further increase of TiO_2 concentration to 0.25 g and 0.5 g onto the $Bi_5O_7NO_3$ surface decreased the adsorption capacity of MO dye. No significant improvement was observed on Ag-modified $Bi_5O_7NO_3$ (BA system). Increased TiO_2 concentration in the presence of fixed amount of Ag particles (TBA system) resulted in an increase in the adsorption capacity of MO dye onto the TBA systems compared to pure $Bi_5O_7NO_3$. The TiO_2 loading was approximately double for all TB and TBA modified adsorbents compared to their calculated values (Table 1). This can be attributed to the different chemical compositions of modified adsorbents and the raw materials from which the adsorbents. Although XRF results imply that TiO_2 particles deposited only on $Bi_5O_7NO_3$ surface, it could not explain the higher adsorption capacity of TBA adsorbents. Samokhvalov et al. (2010) reported that the

Table 1 TiO_2 and Ag loading on modified adsorbents

Sample	BA	TB0.125	TB0.25	TB0.5	TBA0.125	TBA0.25	TBA0.5
XRF analysis							
TiO_2 (wt.%)	None	2.15	4.95	11.54	2.50	4.90	9.60
TiO_2 (g/10 g)	None	0.215	0.495	1.154	0.250	0.490	0.960
AAS analysis							
Ag (mg/10 g)	1.51	None	None	None	3.75	5.13	4.55

wt.% is a mass fraction in g/100 g. BA: Ag-modified $Bi_5O_7NO_3$; TB: introduction of TiO_2 particles on $Bi_5O_7NO_3$ (0.125 g of TB0.125, 0.25 g of TB0.25 and 0.5 g of TB0.5.). TBA: introduction of TiO_2 on $Bi_5O_7NO_3$ in the presence of fixed amount of Ag particles (0.125 g TiO_2 for TBA0.125, 0.25 g for TBA0.25, 0.5 g for TBA0.5).

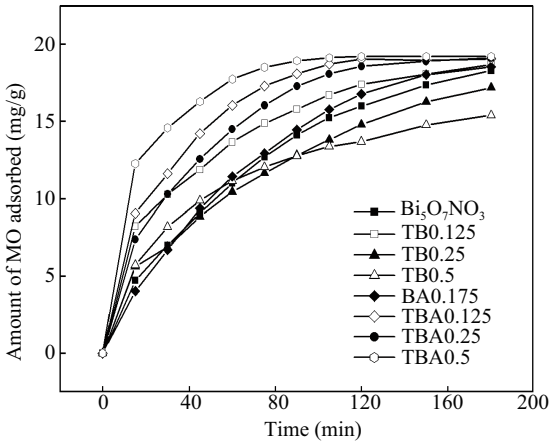

Fig. 1 Evaluation of adsorption performance of various modified adsorbents in removing MO dye from aqueous solution. Experimental conditions: MO 20 mg/L, adsorbent 1.0 g, solution pH 5.7 and (298 ± 1) K.

dispersion of silver particles on TiO_2 surface improved the selective removal of polycyclic aromatic sulphur from liquid hydrocarbon fuels. The highest dispersion of silver particles on TiO_2 adsorbent surface was achieved at Ag/Ti atomic ratio of 0.35. This finding implied that the presence of Ag particles was the main reason for higher adsorption capacity of TBA adsorbents and the highest adsorption capacity of TBA0.5 may be attributed to highly dispersed Ag particles. However, only trace concentrations of Ag were detected by AAS analysis (Table 1). The low concentration of Ag in BA adsorbent compared to TBA adsorbents indicates the low affinity of $Bi_5O_7NO_3$ towards Ag particles. This is in agreement with the observations by Mihailovic et al. (2011), where hydrophilic TiO_2 particles made the $Bi_5O_7NO_3$ surface more hydrophilic and thus facilitating subsequent interaction with hydrophilic Ag particles. However, the trend was independent on TiO_2 concentration.

Due to the higher adsorption capacity of TBA0.5 adsorbent, an emphasis was focused on its structural characteristics as well as on the evaluation of its adsorption performance in the following subsections. The potential use of TBA0.5 for a wide range of azo dyes was determined using SY dye as a model with di-sulphonated azo dyes in aqueous solution.

2.2 Characterization

2.2.1 X-ray diffraction of TBA0.5 adsorbent

Figure 2 illustrates the X-ray diffraction pattern of TBA0.5 adsorbent. The major diffraction lines could be indexed based on orthorhombic structure of $Bi_5O_7NO_3$ (ICDD No. 00-051-0525). Additional peaks belonging to Bi_2O_3 monoclinic phase were discerned at 2θ = 23.18°, 35.10°, 48.40°, 51.30°, 63.95° and 65.16°. Meanwhile, minute traces of uncalcined samples were also detected. There were no characteristic XRD patterns for any polycrystalline formed between $Bi_5O_7NO_3$ and TiO_2. This implies that TiO_2 cannot substitute the Bi^{3+} in the crystal lattice, which is probably attributed to the low calcination temperature, but was only deposited on the $Bi_5O_7NO_3$ surface. TiO_2 peaks were not clearly seen in the XRD pattern. However, with careful observation, the overlapping behaviour can be detected. Anatase peak was observed at 2θ = 25.52° while the rutile peak overlapped with the main peak of $Bi_5O_7NO_3$ at 2θ = 27.67°. Similar overlapping behaviour was observed by Neppolian et al. (2010) with $ZrTiO_4/Bi_2O_3$. XRD pattern for silver was not observed due to its low concentration (5% mol). The crystallite size calculated from the diffraction line of 314 using Debye-Scherer equation was about 35.6 nm.

The surface area, pore volume and radius were found to be 3.9 m^2/g, 0.119 cm^3/g and 19.2 Å, respectively. The increase in surface area of TBA0.5 adsorbent compared to $Bi_5O_7NO_3$ (1.6 m^2/g) indicates the ability of TiO_2-Ag system to slow the thermal decomposition of TBA0.5 adsorbent and inhibit the formation of larger particles. The bigger pore volume and diameter of TBA0.5 compared to that of $Bi_5O_7NO_3$ (0.033 cm^3/g and 17.1 Å, respectively) indicate a considerable amount of surface area in the mesopore region (Long et al., 2005). However, a direct comparison with synthesized carbons showed that

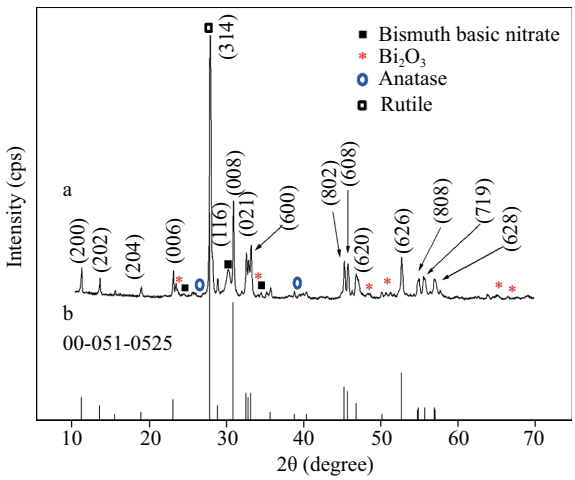

Fig. 2 XRD pattern of TBA0.5 sample at 450°C (line a) and the ICDD-00-051-0525 is included for comparison (line b).

the TBA0.5 is a highly crystallized macro or nonporous material.

2.2.2 Thermogravimetric analysis (TGA) of TBA0.5 adsorbent

The thermogravimetric curve of TBA0.5 showed two major decomposition stages (Fig. 3). The weight loss of 2.8% at 452°C corresponding to the release of NO group from thermal decomposition of $Bi_5O_7NO_3$, indicating that the modified sample may undergo the same decomposition mechanism as described on Reaction (2) (Kodama, 1994b). However, the weight loss arising from oxygen evolution was not observed. The evolved oxygen may be gained by Ag^{2+} species. This conclusion was supported by the finding of Samokhvalov et al. (2010) who showed the presence of minor concentration of Ag^{2+} species on calcined TiO_2 sample at 450°C in air. However, Wang and Yeh (1989) reported that at higher temperature (> 250°C) the oxygen desorption was enhanced by the interaction between $Ag^{2+}O^{2-}$ species and metallic silver surface. This finding suggests that the evolved oxygen may be adsorbed at the defects of TiO_2 surface. The 0.87% weight loss at 354°C may be attributed to the presence of basic bismuth nitrate impurities.

$$Bi_5O_7NO_3 \longrightarrow \frac{5}{2}Bi_2O_3 + NO + \frac{3}{4}O_2 \quad (2)$$

2.2.3 Surface chemistry

For a better understanding of the differences in the structure and surface chemistry of TBA0.5 compared to pure $Bi_5O_7NO_3$, a detailed study of the valence states of the elements detected was performed using XPS. The Bi 4f core level spectrum consisted of double components for Bi $4f_{5/2}$ and Bi $4f_{7/2}$ peaks (Fig. 4a). The corresponding peaks located at binding energies of 164.1 and 158.8 eV could be attributed to Bi $4f_{5/2}$ and Bi $4f_{7/2}$ in TBA0.5, respectively. The shoulders appearing at binding energies of 165.9 and 160.6 eV were assigned to Bi $4f_{5/2}$ and Bi $4f_{7/2}$ orbital's of bismuth basic nitrate impurities, respectively. The binding energies were consistent with those reported in Bi_2O_3 (Xu et al., 2011), indicating the presence of trivalent oxidation state of bismuth centre in TBA0.5 adsorbent.

The observed peak broadening of O 1s core level at binding energy of 531.6 eV (Fig. 4b) indicates the presence of high oxygen content on the TBA0.5 surface, which was probably due to the existence of nitrate (NO_3^-) groups (Watkins et al., 2004).

The Ti 2p core level photoemission peak of TBA0.5 adsorbent overlapped with the Bi $4d_{3/2}$ core level peak (Fig. 4c). By careful deconvolution, the binding energies of Ti $2p_{1/2}$ and Ti $2p_{3/2}$ were observed at 463.8 and 457.6 eV, respectively. The lower binding energy of Ti $2p_{3/2}$ suggests the octahedral coordination of titanium ion on TBA0.5 and segregation of TiO_2 particles on the adsorbent surface (Nocun et al., 2005). In addition, the chain structure of octahedral coordinated titanium ions implies the increase of Ti content which enhances the hydrophilic properties of the surface and creates more positive centres (Capel-Sanchez et al., 2005). Compared to $Bi_5O_7NO_3$, there were no noticeable differences in the chemical states of TBA0.5 adsorbent after the modification process. However, presence of hydrophilic centres was confirmed.

To describe the ionization forms of surface functional groups on the TBA0.5 surface and their interactions with the dye structure, the pH at which the total surface charge is zero (point of zero charge) was determined using the drift equilibrium method. The point of zero charge (pH_{pzc}) of TBA0.5 was found to be 9.5. A comparative study on pH_{pzc} of TBA0.5 and $Bi_5O_7NO_3$ (9.7) clearly showed that the pH_{pzc} value remained constant, implying that the acid/base character of TBA0.5 did not change after the modification process.

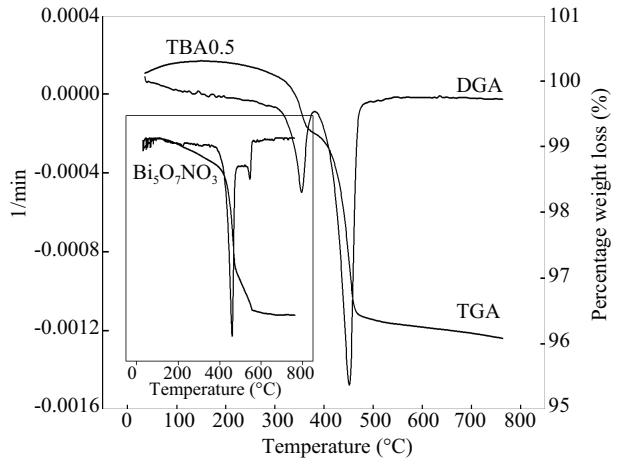

Fig. 3 Thermogravimetric analysis of TBA0.5 adsorbent.

2.3 Adsorption study

2.3.1 Effect of experimental conditions

Adsorption of 20 mg/L MO and SY dyes on TBA0.5 was achieved by dosage 0.75 and 1.0 g, respectively (Fig.

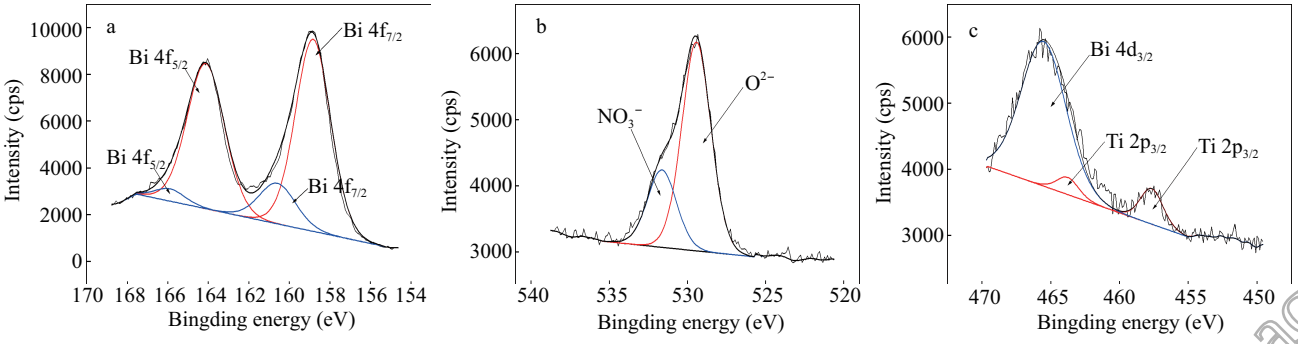

Fig. 4 High resolution XPS spectra of TBA0.5 adsorbent Bi 4f (a), O 1s (b) and Ti 2p (c) core levels.

5a). The increase in dye removal with an increase of adsorbent dose was due to rapid increase in the surface area and the greater number of available binding sites on TBA0.5. No significant difference in MO dye removal was observed at the higher adsorbent doses. However, at high concentration of TBA0.5, the inter-particle interaction such as aggregation led to a decrease in the total surface area available for SY dye removal (Kannan and Veemaraj, 2009).

To obtain maximum adsorption capacity of dye removal on TBA0.5, the effect of initial dye concentration in the range of 10–40 mg/L was studied (Fig. 5b). An increase in initial dye concentration led to an increase in the adsorption capacity until a maximum adsorption was attained at around 25 and 30 mg/L for MO and SY dyes, respectively. This may be due to the adsorbent surface being fully covered by adsorbed dye molecules and also as a result of limited number of available active sites to adsorb highly concentrated dye solution (Abechi et al., 2006). The low adsorption capacity of SY dye could be attributed to the presence of two sulphonate groups on dye structure that significantly enhance the dye's solubility in water and assist the flat orientation of dye molecules leading to decrease in the surface area available for adsorption. The ability of modified adsorbent to disaggregate SY dye molecules was not confirmed, which make the aggregation ability of SY dye molecules as another reason for the low adsorption capacity of SY dye.

The adsorption of MO dye was highly dependent on solution pH suggesting that the electrostatic interaction plays an important role on dye removal (Fig. 5c). Considering the pH_{pzc} of TBA0.5 at 9.5, the lower adsorption capacity at pH 3 can be attributed to the columbic repulsions between protonated MO dye molecules and positively charged surface TBA0.5. The high adsorption capacity occurring at pH range of 6–8 can be attributed to the existence of high electrostatic attraction between anionic dye and the positively charged surface of TBA0.5. The reduction in the adsorption capacity at pH above 8 was due to the competitive adsorption between hydroxyl ions and anionic dye and the electrostatic repulsion between the anionic dye and negatively charged surface of TBA0.5 at pH 10. Similar behaviour was observed for SY dye removal but with a little affinity.

The endothermic or exothermic nature of ongoing adsorption process was studied at different solution temperatures. The adsorption capacities of MO dye onto TBA0.5 increased with an increase in the solution temperature indicating that the adsorption process was endothermic (Table 2). This can be attributed to the endothermic nature of the diffusion process which arises from an increase in dye molecule mobility and a decrease in diffusion resistance forces (Wong et al., 2009). However, the efficiency of SY dye uptake behaviour decreased when the temperature increased due to the decrease in adsorbent-adsorbate interactions that increased the escaping tendency of dye molecules into the solution phase (Fontecha-Camara et al., 2006).

To describe the degree of freedom of the molecules in the system, the thermodynamic parameters, ΔG^{o}, ΔH^{o} and ΔS^{o} of the adsorption process were calculated using Eqs. (3) and (4) (Hanafiah et al., 2012):

$$\Delta G^{o} = -RT\ln K_{c} \quad (3)$$

$$\ln K_{c} = \frac{\Delta S^{o}}{R} - \frac{\Delta H^{o}}{RT} \quad (4)$$

where, ΔG^{o} is the change on Gibbs free energy, ΔH^{o} is the enthalpy, ΔS^{o} is the entropy, R (8.314 J/(mol·K)) is the universal gas constant , T (K) is the reaction temperature in, and K_c is the thermodynamic adsorption equilibrium constant that can be calculated from Eq. (5):

$$K_{c} = \frac{C_{solid}}{C_{liquid}} \quad (5)$$

where, C_{solid} (mg/L) and C_{liquid} (mg/L) are the equilibrium concentration of solute on the surface of adsorbent and solute in the solution.

The negative values of Gibbs energy of MO dye removal increased with an increase in solution temperature strongly suggest that the adsorption process was spontaneous and more favourable at higher temperatures (Table 2). The positive value of ΔH^{o}, indicates the endothermic nature of dye removal. The positive value of ΔS^{o}, indicates the lower order of adsorption process at higher temperatures. However, the enthalpy change in case of SY dye was negative, indicating that the adsorption process was exothermic and may occur due to weak interactions. The negative value

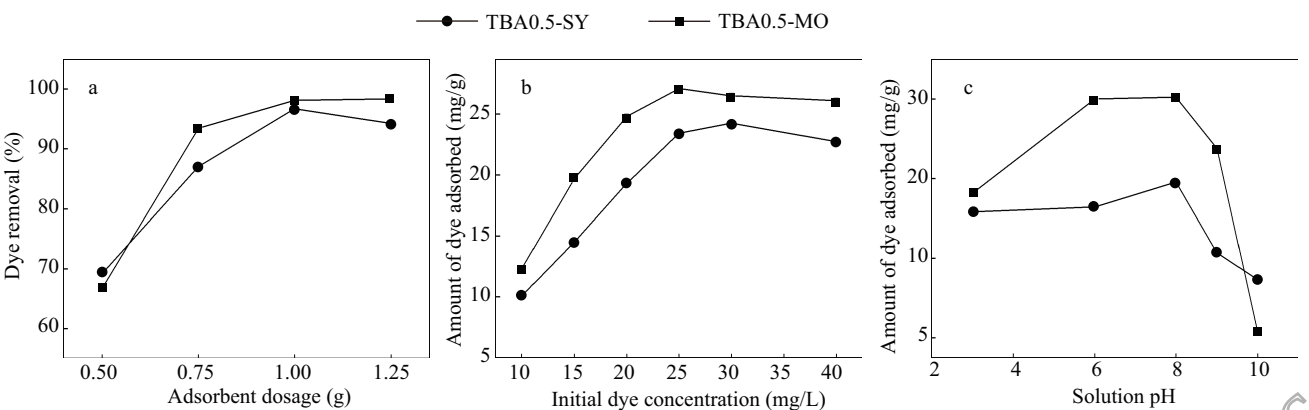

Fig. 5 Adsorption study of MO and SY dye removal onto TBA0.5 adsorbent. (a) effect of adsobent dosage; (b) effect of initial dye concentration; (c) effect of initial solution pH.

Table 2 Thermodynamic parameters of MO and SY dyes adsorption onto TBA0.5 adsorbent

Temperature (K)	R (%)	Q (mg/g)	ΔG^o (kJ/mol)	ΔH^o (kJ/mol)	ΔS^o (J/(mol·K))
MO dye					
298	59.95	24.25	–0.999		
313	78.31	31.99	–3.34	44.7	153.3
333	90.88	36.67	–6.37		
SY dye					
298	84.32	24.99	–4.17		
313	80.93	24.28	–3.76	–35.53	–9.74
333	57.02	17.11	–0.783		

R is the percentage of dye removal, Q is the amount of dye adsorbed on the adsorbent surface at equilibrium

of entropy shows the decrease in randomness at the solid-liquid interface during the adsorption process.

2.3.2 Adsorption isotherm

The distribution of dye molecules between the liquid phase and the adsorbent as a measure of the equilibrium of adsorption process were modelled using Freundlich and Langmuir isotherm (Eqs. (6) and (7)) (Pérez et al., 2007; Zawani et al., 2009). The correlation coefficients were used to clarify the applicability of the model to fit the experimental data.

$$\log Q_e = \log K_F + \frac{1}{n}\log C_e \tag{6}$$

$$\frac{C_e}{Q_e} = \frac{1}{Q_{max}}C_e + \frac{1}{K_L Q_{max}} \tag{7}$$

Freundlich parameters were calculated by plotting $\log Q_e$ versus $\log C_e$ which yields a straight line with a slope of $1/n$ and an intercept of $\log K_F$. Langmuir constants were calculated by plotting C_e/Q_e versus C_e which yields a straight line with a slope of $1/Q_{max}$ and an intercept of $1/K_L Q_{max}$. The shape of the adsorption isotherm was described using a separation factor, R_L (Eq. (8)):

$$R_L = \frac{1}{1 + K_L C_o} \tag{8}$$

where, Q_e (mg/g) is the equilibrium loading on the adsorbent, K_F (mg/g)(L/mg)$^{1/n}$, is the adsorption capacity at unit concentration $1/n$ is the adsorption intensity (heterogeneity factor), C_e (mg/L) is the equilibrium concentration in the dye solution, Q_{max} (mg/g) is the maximum adsorption capacity for complete monolayer, K_L is the Langmuir isotherm constant, and C_o (mg/L) is the initial concentration of the adsorbate.

The higher regression coefficients of Langmuir plots, R^2 = 0.999 and 0.998 for MO and SY dyes adsorption, respectively, indicate the capability of this isotherm to fit the experimental data and the possibility of monolayer coverage of adsorbed dye molecules on the homogenised surface of TBA0.5. The maximum adsorption capacities were found to be 26.2 and 23.3 mg/g for MO and SY dyes, respectively. The R_L values were in range of 0–1, indicating that the adsorption process was more favourable with higher initial concentration of dyes.

2.3.3 Kinetic and diffusion studies

According to Langmuir, adsorption process is a reversible process between adsorbent and adsorbate. The overall adsorption rate is the combination of the first-order term $k_1(1–F)$ and the second-order term $k_2Q(1–F)^2$ (Liu and Shen, 2008). Hence, the Langmuir kinetic represents a hybrid rate equation with a variable reaction order of 1–2. The Langmuir rate equation expression can be written as:

$$\frac{dF}{dt} = k_1(1 - F) + k_2 Q(1 - F)^2 \tag{9}$$

where, k_1 and k_2 represent the rate coefficients of first- and second- kinetic order, respectively, and F is the dimensionless adsorption progress (fractional attainment of equilibrium):

$$F = \frac{Q_t}{Q} \tag{10}$$

This hybrid order is dependent on the adsorption coverage making the analysis more difficult. Thus a simplification in the kinetic description was made by Marczewski (2010) based on adsorption progress (Eq. (11)).

$$\frac{dF}{dt} = (k_1 + k_2 Q)[f1(1 - F) + f_2(1 - F)^2] \tag{11}$$

The integrated form of the Langmuir equation can be written as:

$$\ln\left(\frac{1 - F}{1 - f_{eq}F}\right) = -k_{ia}t \tag{12}$$

where, f_1 and f_2 represent the contribution coefficients of first and second kinetic order, respectively, f_{eq} is Langmuir batch equilibrium factor and k_{ia} is the apparent rate constant of adsorption process. The relative weights of first-order and second-order terms govern the approximation of Langmuir rate equation to first-order or second-order kinetics. Liu and Shen (2008) described this simplification by two parameters: first was the value of the equilibrium coverage fraction θ_e which is given by the following Eq. (12):

$$\theta_e = \frac{K_L(Q_{max}X + C_o) + 1 - \sqrt{K_L^2(C_o - Q_{max}X)^2 + 2K_L(C_o + Q_{max}X) + 1}}{2K_L Q_{max}X} \tag{13}$$

where, X is the adsorbent dosage, and C_o is initial concentration of dye.

The second parameter was the ratio between first-order and second-order rate constants (Eq. (14)).

$$\frac{k_1}{k_2} = \frac{\sqrt{K_L^2(C_o - Q_{max}X)^2 + 2K_L(C_o + Q_{max}X) + 1}}{K_L Q_{max}X} \tag{14}$$

At $k_1/k_2 \geqslant \theta_e$, the Langmuir equation can be reasonably reduced to first-order rate equation, while if $k_1/k_2 \ll \theta_e$, the adsorption kinetic can be described by a second-order rate equation. In the case of k_1/k_2, it is neither close to zero nor close to θ_e, the Langmuir kinetic cannot be simplified

to the first-order or second-order and the adsorption needs to be described by the Langmuir kinetics with a varying reaction order of 1–2.

The Lagergren's first-order and Ho and Mckay pseudo-second rate equations are described in Eqs. (15) and (16).

$$\ln(q_e - q_t) = \ln q_e - k_1 t \quad (15)$$

$$\frac{t}{q_t} = \frac{1}{k_2 q_e^2} + \frac{1}{q_e} t \quad (16)$$

The slope of the straight line in $\ln(q_e - q_t)$ versus t plots was used to determine k_1 value. A linear plot of t/q_t versus t, with $1/q_e$ and $1/k_2 q_e{}^2$ as slope and intercept, respectively, was used to obtain the pseudo-second order rate constants k_2.

The correlation coefficient, R^2, has been commonly used to compare how good the kinetic model is for describing the experimental data; however, the too small differences may prevent any firm conclusion. Thus, the relative goodness of curve fitting, f, which is based on the prediction error square, is used as statistical evidence of the suitability of a kinetic model to fit the experimental data (Eq. (17)).

$$f = \frac{(\sigma^2)_{\min}}{\sigma^2} \quad (17)$$

The term σ^2 is given by Eq. (18):

$$\sigma^2 = \frac{\sum (Y_k - \overline{Y}_k)^2}{n_e - p} \quad (18)$$

where, Y_k and $\overline{Y}_k$ are experimental data and regressed values, and n_e and p are numbers of the experimental data and regressed coefficients, respectively, and $(\sigma^2)_{\min}$ is the minimum value among all σ^2 values determined by different kinetic equations (Liu and Shen, 2008).

The kinetic behaviour of dye removal onto TBA0.5 is described in Table 3. Higher correlation coefficients were observed for the pseudo second-order kinetic model for MO ($R^2 \geqslant 0.986$). In addition, the equilibrium adsorption capacities agreed well with the experimental data suggesting the capability of this model to describe MO dye adsorption onto TBA0.5. However, the f values showed that the simplification of Langmuir mixed order kinetic to second-order rate equation were only valid at a narrow range of concentrations. For SY dye, it was clear that the higher correlation coefficient values could be obtained from pseudo-second kinetic model if the fitting analysis was made at lower concentrations of SY dye, while at higher concentrations of dye pseudo-first kinetic model gave a better fit for the adsorption data. The experimental adsorption capacities were in close agreement with that obtained from pseudo-first kinetic model. However, the f values calculated for all kinetic equations suggest that the Langmuir 1,2-mixed order rate equation is the appropriate kinetic model to describe the adsorption process. At higher concentrations very close f values of the first order to Langmuir mixed order provide statistical evidence for simplification towards the first-order rate equation.

To determine the rate limiting step of adsorption process, the experimental data was modelled by intra-particle diffusion model (IPD) (Eq. (19)) (Weber and Morris, 1962):

$$q_t = K_{id} t^{0.5} + C_{boundary} \quad (19)$$

where, K_{id} (mg/(g·min$^{0.5}$)) is the IPD rate constant and $C_{boundary}$ are constants proportional to the extent of the boundary layer thickness.

As shown in Fig. 6, the uptake is low during the first stage implying that the adsorption process mainly occurred due to intra-particle diffusion as a rate limiting step. However, the intra-particle diffusion model showed multi-linearity plots representing different stages in the adsorption process. This indicates that the rate limiting step cannot be solely described by diffusion of adsorbate along mesopore wall surfaces of the adsorbent in a whole adsorption process. The diffusion of dye molecules across the external surface of adsorbent (macropore walls) has some contribution in the initial stage.

2.4 Comparison study

The adsorption performance and adsorption enhancement of TBA0.5 adsorbent were compared with $Bi_5O_7NO_3$ (Fig. 7). TBA0.5 showed higher adsorption capacity compared to $Bi_5O_7NO_3$. The adsorption capacities were in the order of $TBA0.5_{MO}$ > $TBA0.5_{SY}$ > $Bi_5O_7NO_{3MO}$ >

Table 3 Kinetic parameters for MO and SY dyes removal onto TBA0.5 obtained at different concentrations

Conc. (mg/L)	Q_{Epx} (mg /g)	Pseudo first-order kinetic			Pseudo second-order kinetic			Langmuir 1,2-mixed order kinetic			f value		
		Q_{Calc} (mg/g)	k_1 (1/min) $\times 10^{-2}$	R^2	Q_{Calc} (mg/g)	k_2 (g/mg min)$\times 10^{-2}$	R^2	θ_z	k_1/k_2	Predicted kinetics	First	Second	Langmuir
MO													
10	12.3	11.6	11.0	0.996	13.3	18.2	0.999	0.5029	0.5051	First	0.01708	1.00000	0.10900
15	19.7	16.1	4.0	0.935	21.7	4.1	0.998	0.7485	0.2674	Second	0.06020	1.00000	0.04892
20	24.8	16.5	2.4	0.992	26.3	2.9	0.992	0.9451	0.1278	Second	0.31129	1.00000	0.29599
25	27.1	21.5	1.7	0.961	30.3	1.2	0.988	0.9860	0.2995	Second	1.00000	0.81748	0.99941
30	26.4	23.1	1.8	0.975	31.3	0.9	0.991	0.9925	0.5399	Langmuir	1.00000	0.81589	0.99137
40	26.1	20.8	1.8	0.935	29.4	1.2	0.986	0.9961	1.0396	First	0.92327	1.00000	0.81352
SY													
10	10.1	9.5	5.7	0.994	12.3	0.059	0.998	0.4255	0.5832	Langmuir	0.25393	1.00000	0.92073
15	14.5	14.7	2.3	0.950	17.8	0.015	0.965	0.6351	0.3786	Langmuir	0.45433	0.36081	1.00000
20	19.3	23.2	2.0	0.919	27.0	0.50	0.958	0.8334	0.1966	Second	0.99983	0.39057	1.00000
25	23.4	26.9	1.5	0.899	38.5	0.20	0.844	0.9583	0.1614	Second	0.99998	0.15647	1.00000
30	24.3	25.8	1.2	0.904	38.5	0.19	0.779	0.9838	0.3249	Second	0.99970	0.06544	1.00000
40	22.8	23.9	1.0	0.891	37.0	0.18	0.657	0.9932	0.7354	Langmuir	0.99886	0.03473	1.00000

Q_{Epx} is the experimental value of amount of dye adsorbed at equilibrium time, Q_{Calc} is the calculated value from kinetic model of amount of dye adsorbed at equilibrium time.

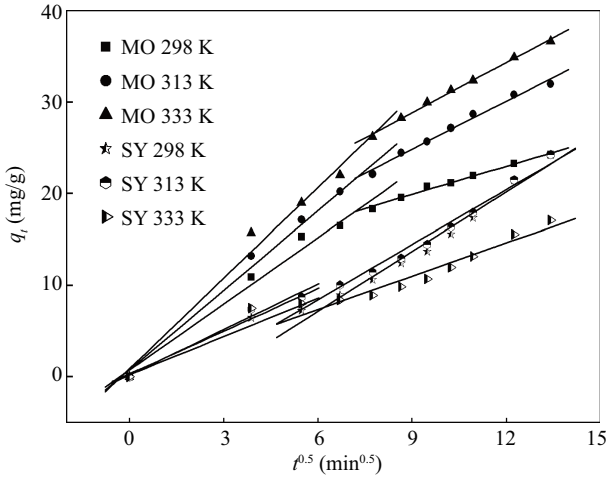

Fig. 6 Intra-particle diffusion plots of MO and SY dyes removal onto TBA0.5 adsorbent at different temperatures.

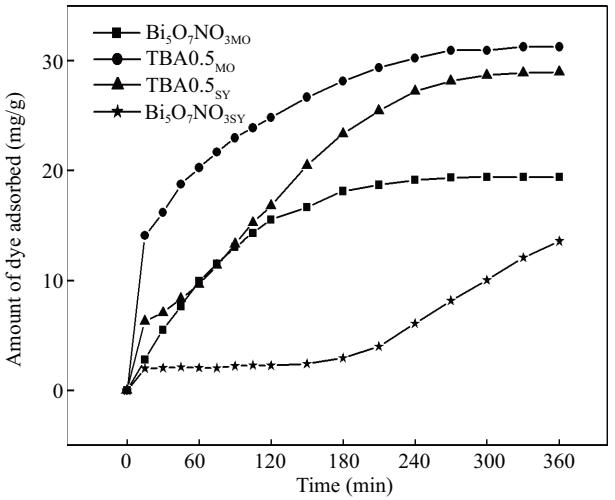

Fig. 7 A comparison study between TBA0.5 and $Bi_5O_7NO_3$ for MO and SY dyes removal.

$Bi_5O_7NO_{3SY}$. The high adsorption capacities of TBA0.5 can be attributed to high surface area, diameter and ultra pore volume as compared with that reported for $Bi_5O_7NO_3$, which indicates that the texture characteristics of TBA0.5 plays an important role in determining the adsorption capacity. The presence of octahedral TiO_2 developed the hydrophilicity characteristic of TBA0.5 surface due to the ability to produce a positively charged surface (Ti^{IV}—OH_2^+) (Asuha et al., 2010). Samokhvalov et al. (2010) and Gan et al. (2004) had suggested that the active species of silver on the calcined TiO_2 sample at 450°C were Ag metal with a minor concentration of Ag^{2+}, which act as hydrophilic centres to develop the positive charge on TBA0.5 surface and enhance the electrostatic attraction with anionic dye molecules.

3 Conclusions

$Bi_5O_7NO_3$ surface was successfully modified by three different modification agents including TiO_2 and/or $AgNO_3$ particles. Surface characterization results revealed that the development of positively charged surface of TBA0.5 as a result of the presence of the hydrophilic centres in combination with the change in surface texture properties of $Bi_5O_7NO_3$ played a vital role in improving and facilitating the adsorbability of MO and SY dyes on TBA0.5 surface. The amount of dye adsorbed varied significantly with adsorbent dosage, initial dye concentration, pH and temperature. The linear regression isotherm of Langmuir provided a better option for describing the experimental data. Although the adsorption kinetic of MO dye could be successfully described by pseudo-second order rate equation, the simplification towards pseudo-first order provides a better understanding of the adsorption kinetic of SY dye onto TBA0.5 adsorbent.

Acknowledgments

The authors are grateful to Taiz University, Yemen for the financial support of Eshraq's scholarship.

References

Abechi S E, Gimba C E, Uziaru A, Ndukwe I G, 2006. Comparative studies on adsorption of methylene blue (MB) by sawdust and walnut shells carbon coated with ZnO. *Science World Journal*, 1(1): 33–35.

Abdullah A H, Abdullah E A, Zainal Z, Hussein M Z, Ban T K, 2012. Adsorptive performance of penta-bismuth hepta-oxide nitrate, $Bi_5O_7NO_3$, for removal of Methyl Orange dye. *Water Science and Technology*, 65(9): 1632–1638.

Afkhami A, Saber-Tehrani M, Bagheri H, 2010. Modified maghemite nanoparticles as an efficient adsorbent for removing some cationic dyes from aqueous solution. *Desalination*, 263(1-3): 240–248.

Andleeb S, Atiq N, Ali M I, Razi-Ul-Hussnain R, Shafiqe M, Ahmed B et al., 2010. Biological treatment of textile effluent in stirred tank bioreactor. *International Journal of Agriculture and Biology*, 12(2): 256–260.

Anjaneyulu Y, Sreedhara C N, Samuel S R D, 2005. Decolourization of industrial effluents-available methods and emerging technologies – A review. *Reviews in Environmental Science and Biotechnology*, 4(4): 245–273.

Asuha S, Zhou X G, Zhao S, 2010. Adsorption of methyl orange and Cr(VI) on mesoporous TiO_2 prepared by hydrothermal method. *Journal of Hazardous Materials*, 181(1-3): 204–210.

Capel-Sanchez M C, Campos-Martin J M, Fierro J L G, 2005. Influence of the textural properties of supports on the behaviour of titanium-supported amorphous silica epoxidation catalysts. *Journal of Catalysis*, 234(2): 488–495.

Combes R D, Haveland-Smith R B, 1982. A review of the genotoxicity of food, drug and cosmetic colours and other azo, triphenylmethane and xanthene dyes. *Mutation Research*, 98(2): 101–248.

El-Qada E N, Allen S J, Walker G M, 2008. Adsorption of basic dyes from aqueous solution onto activated carbons. *Chemical Engineering Journal*, 135(3): 174–184.

Enomoto N, Kawasaki K, Yoshida M, Li X Y, Uehara M, Hojo J, 2002. Synthesis of mesoporous silica modified with titania and application to gas adsorbent. *Solid State Ionics*, 151(1-4): 171–175.

Fernandes F M, Araújo R, Proença M F, Silva C J R, Paiva M C, 2007. Functionalization of carbon nanofibers by a Diels-Alder addition reaction. *Journal of Nanoscience and Nanotechnolgy*, 7(10): 3514–3518.

Fontecha-Camara M A, Lopez-Ramon M V, Álvarez-Merino M A, Moreno-Castilla C, 2006. About the endothermic nature of the adsorption of the herbicide diuron from aqueous solutions on activated carbon fiber. *Carbon*, 44(11): 2335–2338.

Gan Y J, Cai W P, Fu G H, Hu J J, 2004. Water vapour-induced enhancement of the surface plasmon resonance for Ag nanoparticles dispersed within pores of mesoporous silica. *Journal of Physics: Condensed Matter* 16(13): L201–L206.

Guendy H R, 2010. Treatment and reuse of wastewater in the textile industry by means of coagulation and adsorption techniques. *Journal of Applied Sciences Research*, 6(8): 964–972.

Hanafiah M A K M, Ngah W S W, Zolkafly S H, Teong L C, Majid Z A A, 2012. Acid Blue 25 adsorption on base treated shorea *dasyphylla* sawdust: Kinetic, isotherm, thermodynamic and spectroscopic analysis. *Journal of Environmental Science*, 24(2): 261–268.

Kannan N, Veemaraj T, 2009. Removal of Lead(II) ions by adsorption onto bamboo dust and commercial activated carbons a comparative study. *E-Journal of Chemistry*, 6(2): 247–256.

Kodama H, 1994a. The removal and solidification of halogenide ions using a new inorganic compound. *Bulletin of Chemical Society of Japan*, 67(7): 1788–1791.

Kodama H, 1994b. Synthesis of a new compound, $Bi_5O_7NO_3$, by thermal decomposition. *Journal of Solid State Chemistry*, 112(1): 27–30.

Liu Y, Shen L, 2008. From Langmuir kinetics to first- and second-order rate equations for adsorption. *Langmuir*, 24(20): 11625–11630.

Long C, Lu Z Y, Li A M, Liu W, Jiang Z M, Chen J L et al., 2005. Adsorption of reactive dyes onto polymeric adsorbents: Effect of pore structure and surface chemistry group of adsorbent on adsorptive properties. *Separation and Purification Technology*, 44(2): 115–120.

Marczewski A W, 2010. Analysis of kinetic Langmuir model. Part I: Integrated kinetic Langmuir equation (IKL): A new complete analytical solution of the Langmuir rate equation. *Langmuir*, 26(19): 15229–15238.

Mihailovic D, Saponjic Z, Vodnik V, Potkonjak B, Jovancic P, Nedeljkovic J M et al., 2011. Multifuctional PES fabrics modified with colloidal Ag and TiO_2 nanoparticles. *Polymers Advanced Technologies*, 22(12) 2244–2249.

Neppolian B, Kim Y, Ashokkumar M, Yamashita H, Choi H, 2010. Preparation and properties of visible light responsive $ZrTiO_4/Bi_2O_3$ photocatalysts for 4-chlorophenol decomposition. *Journal of Hazardous Materials*, 182(1-3): 557–562.

Nocun M, Mozgawa W, Jedlinski J, Najman J, 2005. Structure and optical properties of glasses from Li_2O-Bi_2O_3-PbO system. *Journal of Molecular Structure*, 744-747: 603–607.

Patel H, Vashi R T, 2010. Adsorption of crystal violet dye onto tamarind seed powder. *E-Journal of Chemistry*, 7(3): 975–984.

Pérez N, Sánchez M, Rincón G, Delgado L, 2007. Study of the behaviour of metal adsorption in acid solutions on the lignin using a comparison of different adsorption isotherms. *Latin American Applied Research*, 37: 157–162.

Poul M, Jarry G, Elhkim M O, Poul J M, 2009. Lack of genotoxic effect of food dyes amaranth, sunset yellow and tartrazine and their metabolites in the gut micronucleus assay in mice. *Food Chemical Toxicology*, 47(2): 443–448.

Samokhvalov A, Nair S, Duin E C, Tatarchuk B J, 2010. Surface characterization of Ag/Titania adsorbents. *Applied Surface Science*, 256(11): 3647–3652.

Wang Y P, Yeh C T, 1989. Electron spin resonance study of the interaction of oxygen with Ag/SiO_2. *Journal of the Chemical Society*, Faraday Transactions, 85(5): 2199–2210.

Watkins R S, Lee A F, Wilson K, 2004. Li-CaO catalysed tri-glyceride transesterification for biodiesel applications. *Green Chemistry*, 6(7): 335–340.

Weber W J, Morris J C, 1962. Advances in water pollution research: Removal of biologically resistant pollutants from waste waters by adsorption. In: Proceedings of the International Conference on Water Pollution Symposium. Oxford: Pergamon Press, Vol. 2: 231–266.

Wong S Y, Tan Y P, Abdullah A H, Ong S T, 2009. Removal of Basic Blue 3 and reactive orange 16 by adsorption onto quartenized sugar cane bagasse. *The Malaysian Journal of Analytical Sciences*, 13(2): 185–193.

Xu J J, Chen M D, Fi D G, 2011. Preparation of bismuth oxide/titania composite particles and their photocatalytic activity to degradation of 4-chlorophenol. *Transactions of Nonferrous Metals Society of China*, 21(2): 340–345.

Zawani Z, Chuah A L, Choong T S Y, 2009. Equilibrium, kinetics and thermodynamic studies: Adsorption of Remazol Black 5 on the palm kernel shell activated carbon (PKS-AC). *European Journal of Scientific Research*, 37(1): 63–71.

Zbaida S, Stoddart A M, Levine, W G, 1989. Studies on the mechanism of reduction of azo dye carcinogens by rat liver microsomal cytochrome P-450. *Chemico-Biological Interactions*, 69(1): 61–71.

JOURNAL OF ENVIRONMENTAL SCIENCES

Journal of Environmental Sciences (Established in 1989)
Vol. 24 No. 10 2012

Supervised by	Chinese Academy of Sciences	**Published by**	Science Press, Beijing, China
Sponsored by	Research Center for Eco-Environmental Sciences, Chinese Academy of Sciences		Elsevier Limited, The Netherlands
		Distributed by	
Edited by	Editorial Office of Journal of Environmental Sciences (JES) P. O. Box 2871, Beijing 100085, China Tel: 86-10-62920553; http://www.jesc.ac.cn E-mail: jesc@263.net, jesc@rcees.ac.cn	Domestic	Science Press, 16 Donghuangchenggen North Street, Beijing 100717, China Local Post Offices through China
		Foreign	Elsevier Limited http://www.elsevier.com/locate/jes
Editor-in-chief	Hongxiao Tang	**Printed by**	Beijing Beilin Printing House, 100083, China

CN 11-2629/X **Domestic postcode: 2-580** **Domestic price per issue RMB ¥ 110.00**

ISSN 1001-0742